Sub-second Imaging Observations of Decametre Solar Radio Spikes

Daniel L. Clarkson[1], Eduard P. Kontar[1], Nicole Vilmer[2], Mykola Gordovskyy[4], Xingyao Chen[1], Nicolina Chrysaphi[1,3]

[1]University of Glasgow [2]LESIA, Observatoire de Paris [3]Sorbonne Université [4]University of Manchester

Based on Clarkson et al. (2023), ApJ, 33, 946

Radio bursts are routinely emitted in the outer solar corona due to the acceleration of energetic electrons in solar flares and coronal mass ejections (CMEs). Among the many solar radio burst types, radio spikes are likely the shortest with narrow spectral widths, suggested to be produced via plasma[1] or electron-cyclotron maser emission[2]. The sub-second bursts are indicative of rapid, small-scale energy release in the corona[3], yet localising the site of electron acceleration is challenging due to radio-wave propagation effects.

Whilst spikes have been observed for decades, imaging observations are relatively sparse and previously limited to decimeter wavelengths. Using millisecond imaging from the LOw Frequency ARray (LOFAR) between 30-45 MHz, we present spatial analysis of hundreds of solar radio spikes associated with a CME.

Event Overview

Clusters of radio spikes and type IIIb bursts were observed by LOFAR on 2017 July 15 with the majority of spikes occurring after the eruption of a streamer-puff CME[4] in association with a C-class flare near the western limb.

Using the LOFAR Low Band Antenna in tied-array beam observing mode with temporal and spectral resolution of 10 ms and 12.2 kHz, respectively, we analyse 1076 individually resolved spikes between 30-70 MHz, with 421 spikes below 45 MHz used for imaging.

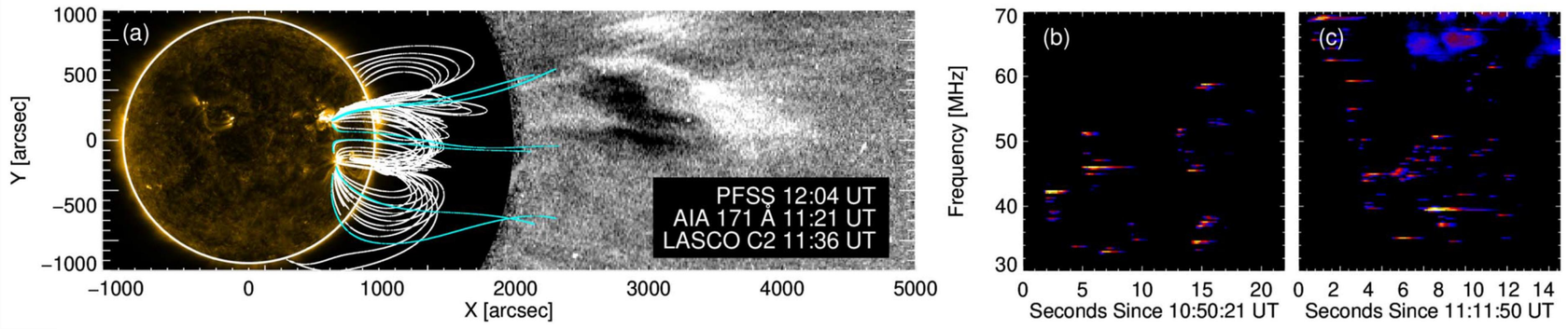

Fig. 1 (above) *Overview of the event on 2017 July 15 showing SDO/AIA 171 Å and LASCO C2 images overlaid with a PFSS extrapolation. The LOFAR dynamic spectra show spike clusters.*

Fig. 2 (below) Left: Normalised time profile (red) of a single spike & the sky-plane y-centroid position. Right: Spike centroid apparent velocities (grey) and their median (blue).

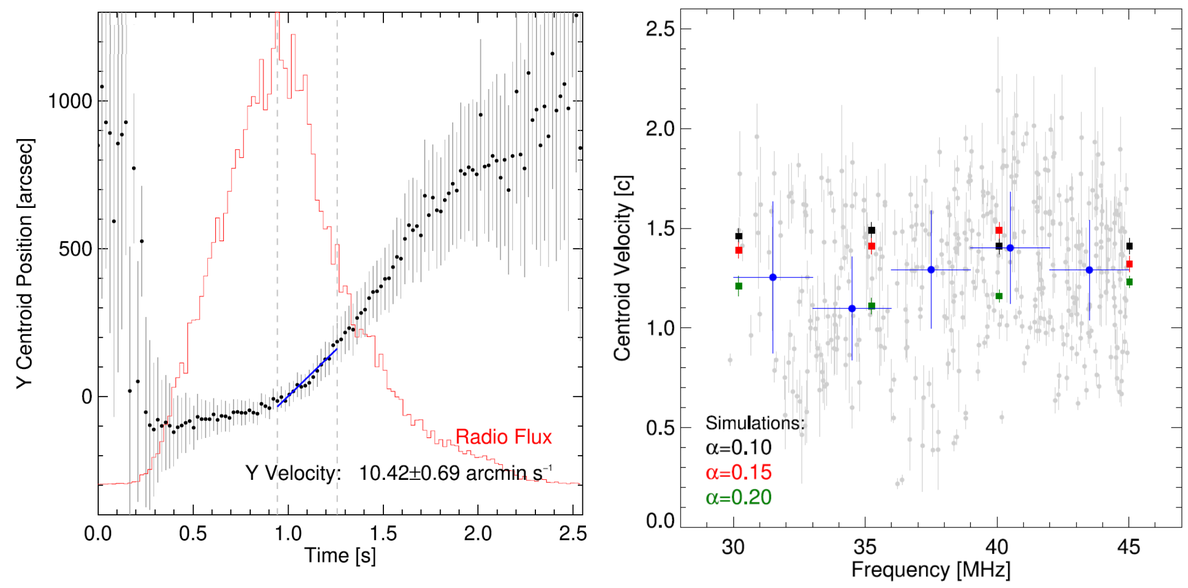

Spike Characteristics & Radio-wave Scattering

Each individual spike displays asymmetric time profiles with decay times of ~0.3 s at 32 MHz. During the decay phase, the spike apparent sizes increase by ~90 arcmin^2 s^{-1} near 32 MHz from a peak area of ~220 arcmin^2. At the same time, the sources drift superluminally across the sky-plane (Fig. 2, 4) parallel to the solar limb.

These characteristics are consistent with significant scattering effects as the radio-waves propagate from the source to the observer[5]. The fast directive motion implies a strong anisotropy[6] of the density turbulence wavevector $\boldsymbol{q}$ between $\alpha = q_{\parallel}/q_{\perp} = 0.1 - 0.2$ ($\alpha = 1$ is isotropic), producing a channelling effect in the direction of the magnetic field such that the ensemble centroid motion traces the magnetic loop structure (Fig. 4).

Emission Timescales

Fig. 3 combines average 1/e spike decay times from several authors up to 1.4 GHz, showing a power-law trend with an index of -1. The trend and amplitude are consistent with scatter broadening such that radio-wave propagation governs the observed decay times, rather than collisional damping.

The intrinsic emission timescale is likely linked to an inhomogeneity time τ on the order of tens of milliseconds, with scales L from $(0.04 - 2) \times 10^4$ km for typical electron beam velocities of $v_b = c/3$.

$$\tau = \frac{|L|}{v_b} = \frac{2n_e(r)}{v_b}\left(\frac{\mathrm{d}n_e(r)}{\mathrm{d}r}\right)^{-1}$$

Fig. 3 (below) Average spike 1/e decay times. Black diagonal lines show plasma collision times. The grey region shows simulated decay time contribution from radio-wave scattering. The red lines show emission timescales due to inhomogeneities with amplitude $\delta n/n$.

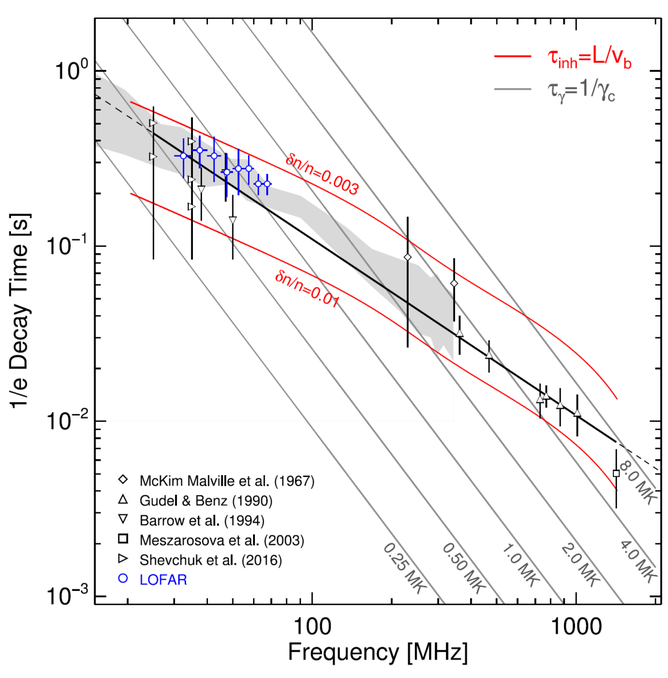

Centroid Motion & Emission Location

The spike apparent sources drift hundreds of arcsec across the sky-plane following the trajectory of a large coronal loop. Consequently, the site of radio-wave emission does not correspond to the observed burst locations and implies acceleration and emission near the CME flank, with emission source sizes $< 1''$ at 30 MHz (inferred from the spike bandwidths).

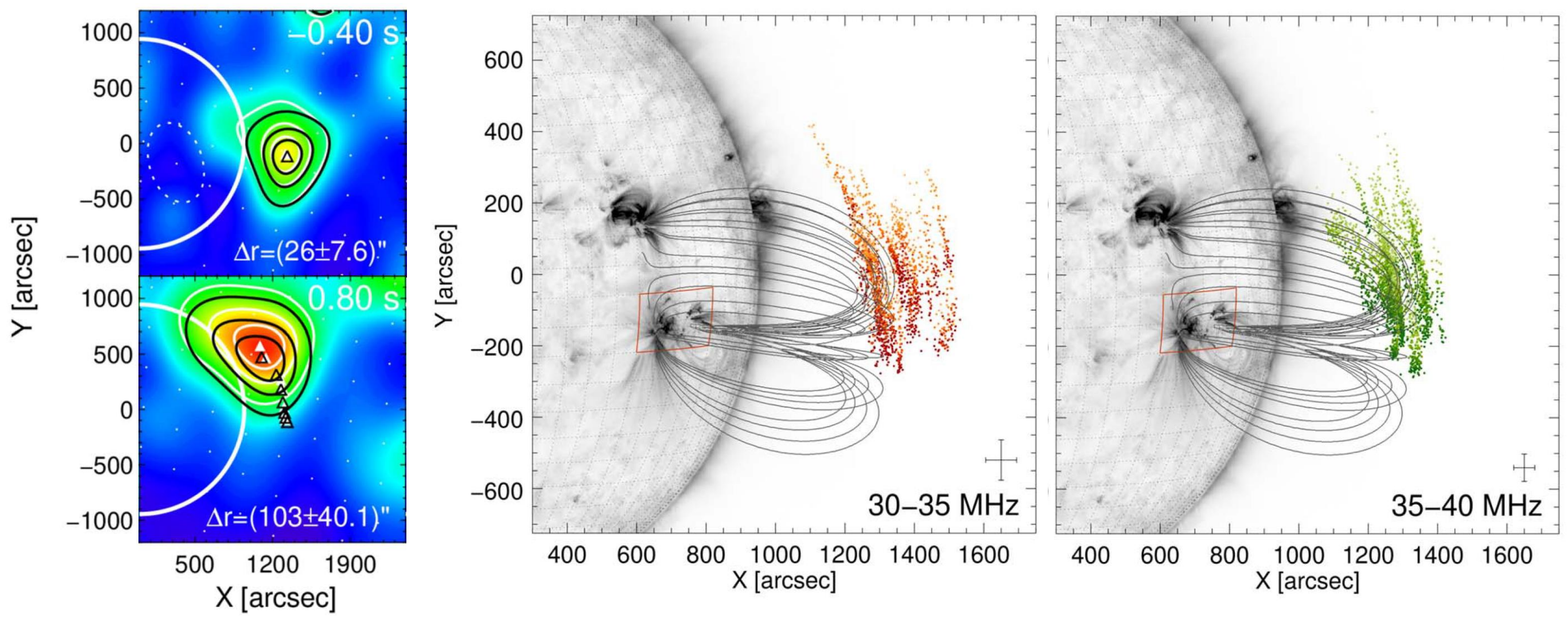

Fig. 4 (above): Left: LOFAR images during the rise and decay phase of a single spike. Centre & Right: Ensemble spike centroid locations over time (dark to light) for two frequency groups.

Conclusion

- LOFAR observations reveal solar radio spikes emitted in association with the passage of a CME.
- Individual spikes exhibit superluminal non-radial motion in the sky-plane & expansion at millisecond scales.
- The temporal & spatial characteristics are consistent with the radiation propagating through strongly anisotropic density turbulence such that the apparent source motion traces the unobserved magnetic field of a closed loop structure.
- Consequently, the observed burst locations do not correspond to the sites of radio emission, indicating that acceleration occurred along the CME flank.
- Disentangling the propagation effects not only offers a unique diagnostic to probe the magnetic field geometry & localise the emission site, but also reveals that the energy release timescales are far shorter and therefore more intense than assumed from observations.

1. Melnik+(2014), SoPh, 289, 1701 **2.** Melrose+(1982), ApJ, 259, 844 **3.** Benz+ (1985), SoPh, 96, 357 **4.** Chrysaphi+(2020), ApJ, 893, 115 **5.** Kontar+(2017), NatCom, 8, 1515 **6.** Kontar+(2019), ApJ, 884, 122